Quantitative Assessment of Gas Hydrates from AVO Crossplot

Kalachand Sain*, Maheswar Ojha and N. K. Thakur
National Geophysical Research Institute, Hyderabad, India

Summary

The most commonly used marker for the investigation of gas-hydrates is the Bottom simulating Reflector (BSR) that is caused by the hydrated sediments underlain by either brine or free-gas saturated sediments. To understand the nature of BSR and to quantify the amount of hydrates and/or free-gas across the BSR, we theoretically compute the AVO intercept (A) and gradient (B) from BSR for various gas-hydrates models. The study demonstrates that the crossplot of A and B attributes can be used as an excellent indicator to detect free-gas below the BSR. We apply the approach to a seismic data in the Makran accretionary prism (Arabian Sea) and the result indicates that the BSR is due to ~10% hydrated sediments underlain by ~5% free-gas saturated sediments.

Introduction

Gas-hydrates have attracted the worldwide attention due to their natural occurrences in the permafrost and outer continental margins; potential as future energy resources, role in climate change and submarine geo-hazards etc. Hence, the identification and quantification of gas-hydrates are very essential to evaluate the resource potential and assess the geohazards. Associated with the base of hydrates stability field is the anomalous bottom-simulating reflector (BSR) on a seismic section, identification of which establishes the presence of gas-hydrates in an area (Hyndman and Spence, 1992; Minshull et al., 1994; Lee et al., 1996; Sain et al., 2000). Seismic reflections from a BSR exhibit a wide range of amplitude versus offset (AVO) characteristics that depends upon the amount of hydrates and free-gas saturations. AVO attributes from the lithologic boundaries have gained considerable popularity for predicting the lithology and reservoir characterization (Castagna and Backus, 1993; Castagna and Smith, 1994; Castagna et al., 1998) but the attributes from a BSR, which is a physical contact between the hydrated sediments above and the brine- or gas-saturated sediments below, have not been exploited properly for the investigation of gashydrates. So we make an attempt to exploit the AVO characteristics for various gas-hydrates models with a view to understand the nature of BSR and to assess the amount of hydrates and/or free-gas. We compute the AVO intercepts (A) and gradients (B) for various hydrates models and demonstrate through a field example that the crossplot of A and B from BSR can be used as an excellent indicator to detect free-gas below the BSR and to quantify the amount of hydrates and/or free-gas.

Theory

The P-wave reflection coefficient, R(q) from a plane interface can be expressed through the AVO intercept, A and the AVO gradient B as a function of incidence angle, q (Shuey, 1985) up to ~30^0 angle as

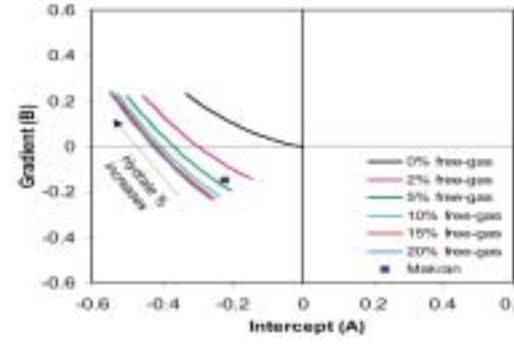

VP, VS and r are the P-wave velocity, S-wave velocity and density respectively. The subscript 1 and 2 represent the top and bottom layers of the interface respectively.

To calculate the P-wave velocity for hydrates bearingsediments, we use the three-phase weighted equation of *Lee et al*. (1996) with weighting factor of W=1.155, exponent N=1 and porosity ϕ= 40%. The S-wave wave velocity of hydrated sediments is calculated using the formula of Castagna et al. (1985) as

$$V_p = 1.16V_s - 1.36 \qquad (5)$$

We calculate the P- and S-wave seismic velocities

for hydrated sediments by changing the concentration of hydrates only keeping fixed values of all other constants as used by Lee et al. (1996). The P- and S-wave seismic velocities of gas-saturated sediments are calculated using the formula of Minshull et al. (1994) by varying the saturation of gas only. Since the density of hydrates or freegas saturated sediment remains unaffected, we use Dr=0 in equation (3).

First we compute the P- and S-wave seismic velocities and then the AVO attributes from a BSR caused by hydrates underlain by brine saturated sediments using the expressions (2) and (3) by varying the saturation of hydrates from 0 to 100% at interval of 5% above and 0% free-gas or 100% brine saturation below the BSR. The crossplot of A and B is displayed in Figure 1, and this is treated as the background to predict free-gas below the BSR. Next we compute the A and B attributes from a BSR caused by hydrated sediments underlain by free-gas bearing sediments by varying the saturation of hydrates from 0 to 100% at interval of 5% with fixed saturation of 2%, 5%, 10%, 15% and 20% free-gas below the BSR. The crossplots are displayed in Figure 1, which shows that the saturation of free-gas above 10% cannot be distinguished from each other based on AVO attributes whatever the saturations of hydrates are. The figure also shows that the crossplot of A and B for hydrate/brine BSR falls in the 2nd quadrant (negative A and positive B) and passes through the origin with a gradient of ~ 45°. However, the crossplots of A and B deviates clearly from the background trend, even in presence of small amount (<2%) of free-gas. Thus, the crossplot of A and B can be used as an indicator for free-gas below the BSR, irrespective of hydrates saturation. For hydrates/free-gas BSR, both A and B show negative values up to ~50% hydrate saturation, and therefore signifies as a class III type gas sands indicator. For hydrate saturation above 50%, A is large negative and B is positive, which can be classified as an indicator of type IV gas sands (Castagna et al., 1998).

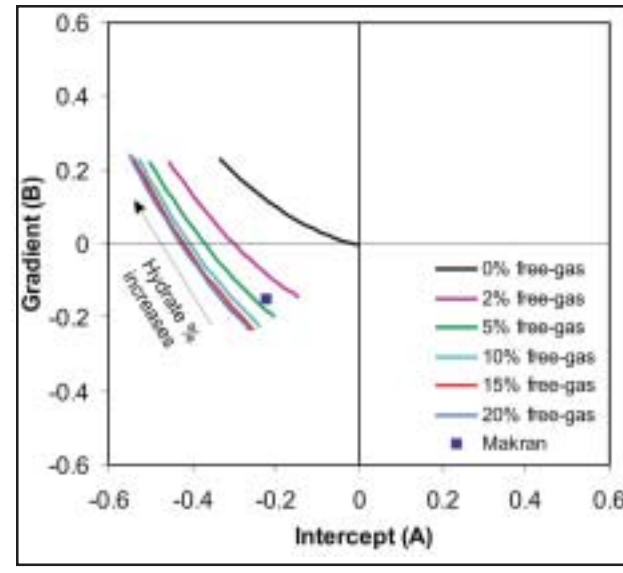

Fig.1: Theoretical crossplots between the AVO intercept, A and the gradient, B for hydrate saturation varying between 0 to 100% with fixed saturation of (i) 0%, (ii) 2%, (iii) 5%, (iv) 10%, (v) 15% and (vi) 20% free-gas.

Example

We compute the AVO attributes from the MCS data in the Makran accresionary prism (Arabian Sea) where widespread occurrences of BSRs have been reported (Sain et al. 2000). The BSR is identified at about 2.8 – 2.9 s TWT on the seismic section (Figure 2a) where water depth is ~1.7 km. The data has 24 folds with maximum offset of 2.56 km. A representative CDP gather at CDP 4380 showing reflections from seafloor and BSR (upper panel), and the first multiple of seafloor reflection (lower panel) is displayed in Figure 2b.

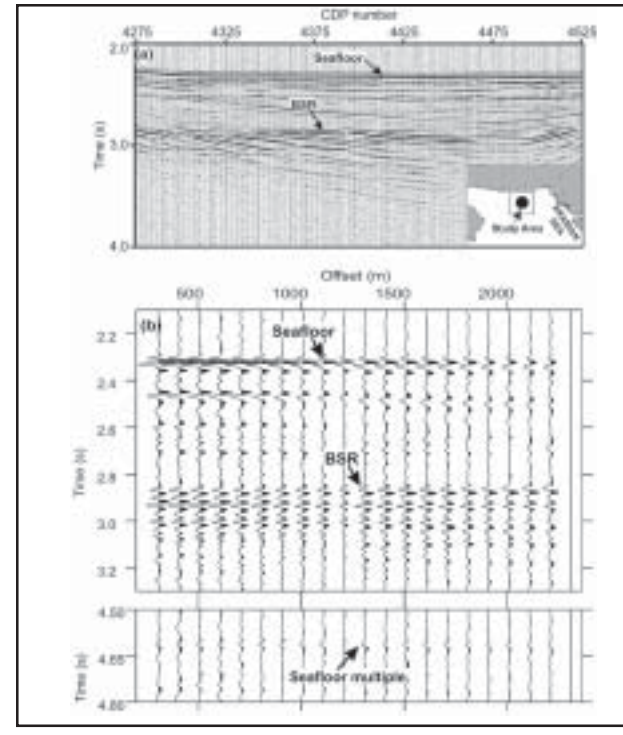

Fig. 2: (a) Seismic section between CDPs 4275 to 4525 in the Makran accretionary prism showing reflections from the seafloor and BSR. Inset shows the study area. (b) Representative NMO corrected CDP gather at CDP 4380 showing reflections with offsets from the seafloor and BSR (upper panel), and the first multiples of the seafloor (lower panel) in the Makran accretionary prism.

The values of A and B for BSR are computed using equation (1). The BSR reflection coefficients, *bsr R* are calculated using the Warner's approach (1990) as

$$R_{bsr} = \frac{A_{bsr}}{A_p} R_s \qquad (6)$$

Where, A_{bsr} = the amplitude of the BSR.
$R_s = A_m / A_p$ = the seafloor reflection coefficient,

A_m = the amplitude of the first multiple of the seafloor reflection,
A_p = the amplitude of the seafloor reflection.

Data are processed and amplitudes of the seafloor, BSR and first multiples of seafloor are picked by using ProMax - a commercial seismic data processing software. The spherical divergence correction is applied to the data before picking amplitudes from NMO corrected CDP gathers. Depth to the BSR is obtained by converting the TWT-RMS velocity function (derived by the velocity analysis) into the velocity-depth function by well-known Dix's formula. To correct the transmission losses at the seafloor, the reflection coefficients of the BSR are multiplied by the factor $1/(1-R^2_s)$ (Fink and Spence, 1999). For the calculation of AVO attributes, we select 100 CDPs from 4350 to 4450 where the BSR is strong. To get reflection coefficients with angle of incidence, offsets are converted into angles as

$$\theta = Sin^{-1}\left(x/\sqrt{(x^2+z^2)}\right) \qquad (7)$$

Where , x and z are the angle of incidence, half-offset and depth to the reflector respectively. Using equation (6), we calculate the reflection coefficients for each trace of the CDP gathers, plot the values against sin2θ and draw the best-fit regression line (Figure3) to determine the A and B attributes shown in Figure 1.

Conclusions

Theoretical calculation of AVO attributes A and B from BSR for various gas-hydrates models demonstrates that the crossplot of A and B can be used as an important tool to detect free-gas below the BSR. The crossplot also indicates that the gas sand beneath the BSR can be interpreted as Class III type gas sand for hydrate saturation up to ~50% and as Class IV type gas sand above 50% hydrate saturation. The estimated A-B value for the BSR in the Makran accretionary prism deviates from the background trend and falls on the 3rd quadrant indicating free-gas below the BSR. From the theoretically calculated nomograms of A-B crossplots, we estimate the amount of hydrates to be 10% underlain by 5% free-gas. More accurate estimation of hydrates and free-gas in the study area is possible, provided we know the porosity, matrix velocity and values of other constants accurately.

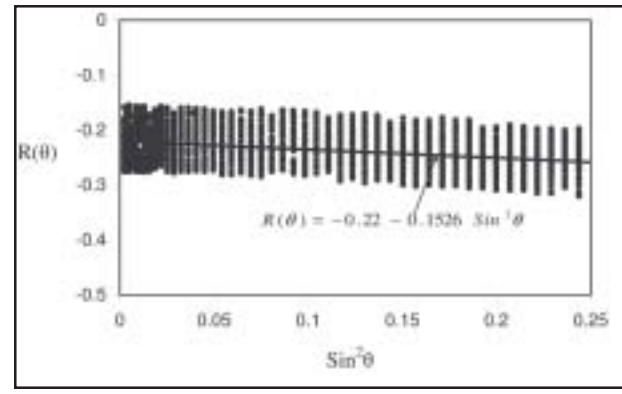

Fig. 3: Reflection coefficients, R() versus Sin2 plots for 100 CDP gathers in the Makran accretionary prism.

References

Castagna, J. P. and Backus, M. M., 1993, Offset dependent reflectivity: Theory and Practice of AVO analysis; Soc. Expl. Geophys.

Castagna, J. P., Batzle, M.L. and. Eastwood, R. L., 1985, Relationships between compressional and shear- wave velocities in clastic silicate rocks; Geophysics, 50, 551 570.

Castagna, J. P., Swan, H. W. and Foster, D. J., 1998, Framework for AVO gradient and intercept interpretation; Geophysics, 63, 948-956.

Fink, C. R. and Spence, G. D., 1999, Hydrate distribution off Vancouver Island from multifrequaency single-channel seismic reflection data; J. Geophys. Res., 104, 2909-2922.

Lee, M. W., Hutchinson, D. R., Collett, T. S. and Dillon, W. P., 1996, Seismic velocities for hydrate-bearing sediments using weighted equation; J. Geophys. Res., 101, 20347-20358.

Hyndman, R.D. and Spence G. D., 1992, A seismic study of methane hydrate marine bottom simulating reflectors; J. Geophys. Res., 97, 6683-6698.

Minshull, T. A., Singh, S. C. and Westbrook, G. K., 1994, Seismic velocity structure at a gas hydrate reflector, offshore western Columbia, from full waveform inversion; J. Geophys. Res., 99, 4715-4734.

Sain, K., Minshull, T. A., Singh, S.C. and Hobbs, R.W., 2000, Evidence for a thick free gas layer beneath the bottom simulating reflector in the Makran accretionary prism; *M*ar. Geol., *164*, 37-51.

Shuey, R. T., 1985, A simplification of Zoeppritz equations; *G*eophysics, 50, 609-614.

Warner, M., 1990, Absolute reflections from deep seismic reflections; *T*ectonophysics, 173, 15-23.

Acknowledgements

We are grateful to the Director, NGRI for his kind consent to publish this work. Department of Science and Technology, Delhi is acknowledged for financial support through an award of Swarnajayanti Project.